Journal of Hepatocellular Carcinoma

Dovepress
Taylor & Francis Group

Open Access Full Text Article

ORIGINAL RESEARCH

Development and Validation of a Nomogram for Predicting Response to TACE Combined with Lenvatinib and Anti-PD-1 Therapy in Unresectable Hepatocellular Carcinoma

Ying Wu[1], Linhui Li[2], Xing Wang[3], Jiandong Shen[4,*], Yanjun Sun[3,*]

[1]Department of Ultrasound, Wuxi Hospital of Traditional Chinese Medicine, Wuxi, Jiangsu, 214000, People's Republic of China; [2]Changzhou Third People's Hospital, Changzhou, Jiangsu, 213000, People's Republic of China; [3]Department of Oncology, Yancheng Tinghu District People's Hospital, Yancheng, Jiangsu, 224000, People's Republic of China; [4]Department of Invasive Technology, Affiliated Nantong Hospital 3 of Nantong University, Nantong, Jiangsu, 226001, People's Republic of China

*These authors contributed equally to this work

Correspondence: Yanjun Sun, Department of Oncology, Yancheng Tinghu District People's Hospital, No. 66 Zhongting Middle Road, Tinghu District, Yancheng, Jiangsu, 224000, People's Republic of China, Tel +86-18105109911, Email 8994518@qq.com

Background: The prognosis for unresectable hepatocellular carcinoma (u-HCC) patients receiving monotherapy remains poor, driving the need for more effective combination therapies. Although transarterial chemoembolization (TACE) combined with targeted therapy and immunotherapy shows promising efficacy, robust biomarkers are needed to identify patients most likely to benefit. This study aimed to develop and validate a nomogram to predict treatment response in u-HCC patients receiving triple therapy.

Methods: We conducted a multicenter retrospective study including u-HCC patients who received triple therapy between January 2021 and June 2024. Patients from one hospital (n=91) were assigned to the training cohort, and those from two other centers (n=54) constituted the external validation cohort. Treatment response was evaluated according to mRECIST criteria. Univariate and multivariate logistic regression analyses were performed to identify independent predictors of the objective response rate (ORR). A nomogram integrating clinical and imaging features was constructed and evaluated using receiver operating characteristic (ROC) curves, calibration plots, and decision curve analysis (DCA).

Results: Multivariate analysis identified six independent predictors of ORR: alpha-fetoprotein (AFP) level, lymphocyte-to-monocyte ratio (LMR), portal vein tumor thrombus (PVTT), tumor number, irregular arterial phase enhancement, and tumor rupture. The combined nomogram, integrating clinical and imaging features, demonstrated superior predictive performance, with AUCs of 0.915 (95% CI: 0.838–0.963) in the training cohort and 0.933 (95% CI: 0.831–0.983) in the validation cohort. Calibration curves showed good agreement between predicted and observed probabilities, and DCA confirmed the clinical utility of the model. The incidence of adverse events did not differ significantly among treatment regimens ($P > 0.05$).

Conclusion: We developed and validated a non-invasive nomogram that integrates readily available clinical and imaging features to effectively predict treatment response to triple therapy in u-HCC patients. This tool holds potential for personalizing treatment strategies and improving prognostic assessment.

Keywords: unresectable hepatocellular carcinoma, transcatheter arterial chemoembolization, lenvatinib, immunotherapy, radiological characteristics, predictive model

Introduction

Hepatocellular carcinoma (HCC) represents the predominant histologic type of liver cancer, comprising approximately 75%-85% of cases. It ranked as the sixth most commonly diagnosed cancer and the third leading cause of cancer-related mortality globally in 2020.[1] The insidious onset of HCC often leads to diagnosis at intermediate or advanced stages,[2] when patients are

https://doi.org/10.2147/JHC.S580139
Received: 20 November 2025
Accepted: 25 January 2026
Published: 2 February 2026

typically ineligible for curative surgical resection. For such patients, the standard of care involves locoregional therapies (eg transarterial chemoembolization) and systemic therapies, primarily encompassing targeted agents and immunotherapeutic drugs. In recent years, research on targeted therapies and immunotherapies for liver cancer has yielded promising results and has seen widespread application in clinical practice. However, for patients with intermediate and advanced liver cancer, the outcomes of TACE or drug therapies alone remain unsatisfactory. As a result, the combination of transarterial chemoembolization (TACE) with targeted therapy and immunotherapy (triple therapy) is being increasingly practiced in clinical treatment for advanced liver cancer, showing favorable outcomes. For example, a study[3] involving 98 patients with intermediate and advanced hepatocellular carcinoma reported that the objective response rate (ORR) of triple therapy reached 56.1%, with a disease control rate (DCR) of 81.6%. The combination therapy was shown to enhance cellular immunity. Although some patients with advanced liver cancer experienced significant survival benefits from the combined treatment, others had poor treatment outcomes.[4] This variability may be attributed to differences in tumor characteristics and immune responses among patients. Additionally, the high cost of combination therapy and the increased incidence of drug-related adverse reactions underscore the importance of early evaluation of clinical efficacy.

Studies have shown that the systemic inflammatory response and the immune status of cancer patients are closely associated with treatment outcomes.[5,6] Most hepatocellular carcinoma (HCC) develops from chronic liver disease, with common causes including viral hepatitis infection, non-alcoholic fatty liver disease, and excessive alcohol consumption.[7] Chronic liver inflammation resulting from liver disease impairs the hepatic immune system, making it easier for tumor cells to evade immune surveillance.[8] In an inflammatory context, cancer cells become surrounded by stromal and immune cells, forming a tumor microenvironment that promotes tumor progression. Previous studies have indicated that inflammatory markers can reflect cancer prognosis. For example, the lymphocyte-to-monocyte ratio (LMR) represents the balance between pro-tumor factors and anti-tumor immune function, with a low LMR being associated with poor prognosis in HCC patients.[9,10]

Additionally, the intrinsic characteristics of the tumor are critical factors influencing the prognosis of HCC.[11] Contrast-enhanced computed tomography (CT) is the preferred imaging method for HCC due to its efficiency and cost-effectiveness.[12] However, while researchers have focused on predicting HCC prognosis based on clinical and hematologic factors, enhanced CT features have not been fully considered. The prognostic significance of enhanced CT characteristics remains to be further established. Compared to a single biomarker, predictive models incorporating multiple biomarkers are more useful.[13] Enhanced CT scans can reveal tumor size, location, rupture, hemorrhage, and the presence of portal vein tumor thrombus (PVTT). For instance, tumor rupture and hemorrhage in liver cancer patients lead to a poor prognosis, with mortality rates as high as 50% to 80%.[14] Additionally, the presence of PVTT promotes intrahepatic tumor spread, limits treatment options, and worsens treatment tolerance in HCC patients.[15]

Therefore, this study aimed to develop and validate a non-invasive model integrating radiological features and systemic inflammatory markers (such as LMR) to facilitate pre-therapeutic identification of u-HCC patients who would derive the greatest benefit from triple therapy, thereby aiding in personalized treatment decision-making.

Methods

Study Population

This multicenter, retrospective study was led by Yancheng Tinghu District People's Hospital and was approved by its Institutional Ethics Committee (Approval No.: 2024-SR-016). The need for informed consent was waived by the same committee due to the retrospective nature of the study. The ethical approval was also acknowledged by the collaborating centers (Affiliated Hospital of Nantong University, Nantong Third People's Hospital, and Nantong Tumor Hospital). We enrolled 145 patients with unresectable hepatocellular carcinoma (u-HCC) who received triple therapy between January 2021 and June 2024. Based on the source institution, the patients were divided into a training cohort (n=91) from the Affiliated Hospital and a validation cohort (n=54) from the other two centers. The inclusion criteria were:

1. Age ≥ 18 years;
2. No prior HCC-related treatment (either local or systemic);

3. Child-Pugh liver function classification of A or B (≤ 9 points);
4. Presence of at least one measurable HCC lesion (according to mRECIST criteria);
5. Pathologically confirmed diagnosis of u-HCC, or clinically diagnosed u-HCC according to the "Guidelines for the Diagnosis and Treatment of Primary Liver Cancer (2024 edition)";
6. Regular treatment with TACE, targeted therapy, and immunosuppressive agents;
7. Complete clinical and imaging data.

The exclusion criteria were:

1. Presence of other primary cancers or metastatic liver cancer;
2. Contraindications to triple therapy;
3. Incomplete clinical or imaging data;
4. Discontinuation of treatment;
5. Prior anti-tumor therapy before the start of observation;
6. Presence of autoimmune diseases.

Clinical and Imaging Data

All patients received TACE combined with targeted and immunotherapy. We retrospectively reviewed the hospital information system to retrieve baseline data one week prior to triple therapy, including gender, age, hypertension, diabetes, hepatitis, cirrhosis, antiviral treatment, Child-Pugh classification, ECOG performance status, and serological and imaging markers. Serological data included lymphocytes, monocytes, neutrophils, platelets, platelet distribution width, red blood cells, red cell distribution width, albumin, fibrinogen, LMR,[16] Neutrophil-to-Lymphocyte Ratio (NLR),[17] Platelet-to-Lymphocyte Ratio (PLR),[18] Systemic Inflammation Response Index(SIRI),[16] Systemic Immune-Inflammation Index(SII),[19] Imaging data included tumor size, number, distribution, morphology, capsule integrity, rupture and bleeding status, PVTT, arterial phase enhancement pattern, and metastatic status.

TACE Procedure

All patients underwent a standardized protocol of transarterial chemoembolization (TACE) performed by experienced interventional radiologists (≥10 years of experience) across all participating centers. Prior to study initiation, a unified TACE operation manual was established and distributed to all centers to ensure procedural consistency. Contraindications included Child-Pugh class C or ECOG score > 2. Under sterile conditions, percutaneous access was achieved via the femoral artery using the Seldinger technique. Angiography was performed to assess tumor vascularity, with additional vessels evaluated if inadequate tumor staining was observed. Superselective embolization was then performed using a 2.7F microcatheter, injecting a Lipiodol-doxorubicin/epirubicin emulsion until complete devascularization was achieved, followed by gelatin sponge embolization. The embolization endpoint was defined as stasis of contrast medium in the tumor-feeding arteries. Postoperative supportive care included liver protection, hydration, and anti-inflammatory management. All TACE procedures were reviewed by an independent interventional radiology panel to confirm adherence to the standardized protocol.

Systemic Therapy

All medications were administered according to predefined, uniform dosing protocols across all centers. Lenvatinib was administered orally at a dose of 8 mg once daily for patients weighing ≤ 60 kg or 12 mg once daily for those > 60 kg. Dose adjustments were permitted only for managing adverse events and followed a predefined protocol. Immunotherapeutic agents—including camrelizumab, sintilimab, and tislelizumab—were administered intravenously at a fixed dose of 200 mg every three weeks. Treatment cycles were synchronized across centers, and all patients received the first dose within one week after TACE. To minimize inter-center variability in supportive care, a standardized management guideline for adverse events was implemented across all participating institutions.

Follow-Up and Outcome Assessment

Patient follow-up included laboratory tests (complete blood count, liver and kidney function, thyroid function, cardiac enzymes, and tumor markers) every 4–6 weeks and imaging examinations (contrast-enhanced abdominal CT and chest CT) at least every 2 months. Two radiologists (with 5–6 years of experience), blinded to clinical data, independently assessed the images. Discrepancies were resolved by consensus. Tumor burden was characterized by number (categorized as single or multiple [>2]) and the longest diameter of the largest lesion.

The primary outcome was the Objective Response Rate (ORR) assessed at the first scheduled imaging evaluation between 4 and 6 months (approximately 16–24 weeks) after initiation of triple therapy. ORR defined as the proportion of patients achieving a Complete Response (CR) or Partial Response (PR) according to mRECIST criteria. CR was defined as the disappearance of any intratumoral arterial enhancement in all target lesions. PR required at least a 30% decrease in the sum of diameters of viable (arterial phase-enhancing) target lesions. Patients with Stable Disease (SD) or Progressive Disease (PD) were classified as non-responders.

Data Analysis

Statistical analyses were performed using SPSS (version 25.0) and R software (version 4.0.5). A two-sided P-value < 0.05 was considered statistically significant. Continuous variables were expressed as mean ± standard deviation or median (interquartile range) based on their normality of distribution, and compared using the independent samples *t*-test or Mann–Whitney *U*-test, respectively. Categorical variables were presented as numbers (percentages) and compared using the Chi-square test or Fisher's exact test, as appropriate. Given the number of candidate predictors relative to the sample size, a two-step variable selection process was employed to mitigate the risk of model overfitting. First, the least absolute shrinkage and selection operator (LASSO) regression method was applied to reduce data dimensionality and select the most relevant features. We employed LASSO regression for variable selection given its suitability for high-dimensional data with limited samples, its ability to prevent overfitting via L1 regularization, and its established utility in clinical prediction modeling. The optimal tuning parameter (λ) was determined via 10-fold cross-validation with the minimum criterion. Subsequently, variables with non-zero coefficients selected by the LASSO regression were included in the univariate logistic regression analysis. Variables achieving a significance level of $P < 0.05$ in the univariate analysis were then entered into a multivariate logistic regression model using the enter method to identify independent predictors of the objective response rate (ORR). Based on the final multivariate model, a predictive nomogram was constructed using the rms package in R. The model's performance was evaluated by assessing its discrimination and calibration. Discrimination, which refers to the model's ability to distinguish between responders and non-responders, was quantified by the area under the receiver operating characteristic curve (AUC). Calibration, which assesses the agreement between predicted probabilities and observed outcomes, was evaluated using calibration plots and the Hosmer-Lemeshow goodness-of-fit test. The clinical utility of the nomogram was further evaluated using decision curve analysis (DCA), which estimates the net benefit across a range of threshold probabilities.

Results

Patient Characteristics

Figure 1 illustrates the patient selection flowchart. Patient characteristics, including clinical parameters and imaging features of both cohorts, are summarized in Tables 1 and 2. The clinical parameters and imaging features were similar between the training and validation cohorts. The detailed medication regimens for both groups are presented in Table 3. These findings suggest that the baseline data of the two cohorts had no significant differences, indicating that they were homogeneous and comparable, providing a solid foundation for subsequent analyses.

Identification of Predictors for Treatment Response

Given the analysis of nearly 40 variables and a limited training cohort of 91 patients, LASSO regression was applied to reduce data dimensionality and mitigate overfitting risks. As illustrated in Figures 2A and B, at the optimal lambda value ($\lambda = 0.048$), eight predictors were selected: AFP level, tumor number, tumor rupture, PVTT, metastasis, irregular arterial enhancement, RDW, and LMR.

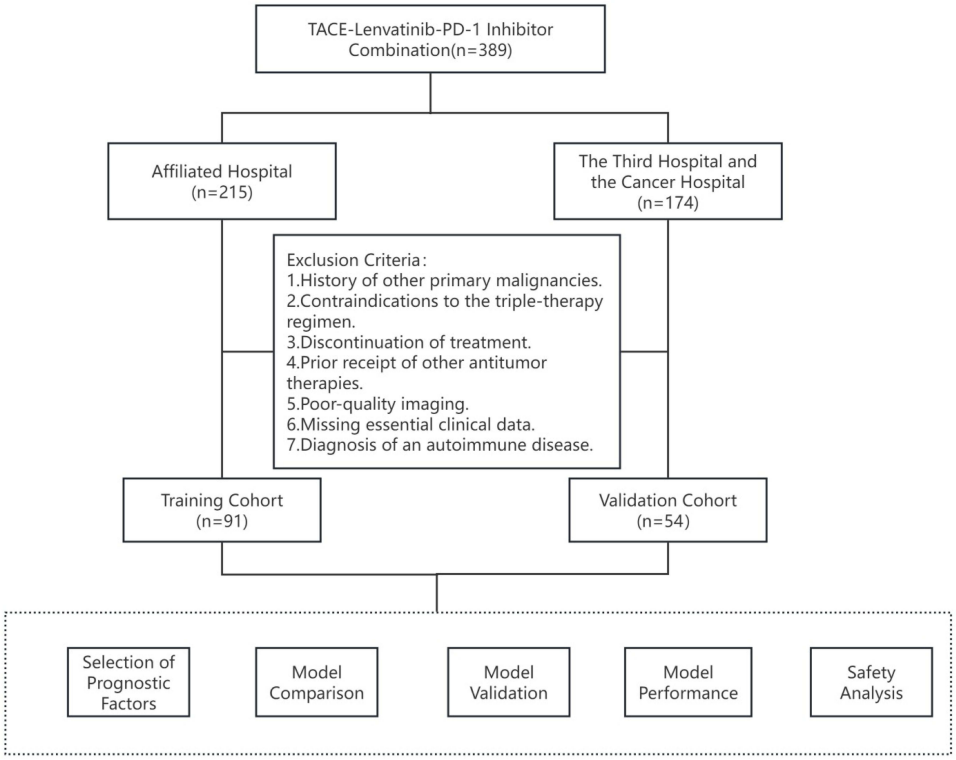

Figure 1 The study flowchart.

Univariate analysis (Table 4) identified LMR, AST, AFP level, tumor number, tumor rupture, PVTT, and irregular arterial enhancement as significantly associated with treatment response. Integrating the results from both LASSO regression and univariate analysis, the following key variables were ultimately determined as major predictors of triple-therapy outcome: AFP level, tumor rupture, tumor number, LMR, irregular arterial enhancement, and PVTT.

Table 1 Baseline Characteristics of the Study Population

	Total (n = 145)	Training Set (n = 91)	Validation Set (n = 54)	Statistic	P
Age (years)	63.14 ± 10.31	62.62 ± 11.62	64.02 ± 7.61	t = −0.88	0.382
Gender (%)				χ^2 = 0.54	0.462
Male	122 (84.14)	75 (82.42)	47 (87.04)		
Female	23 (15.86)	16 (17.58)	7 (12.96)		
Child-Pugh				χ^2 = 3.02	0.082
A	91 (62.76)	62 (68.13)	29 (53.70)		
B	54 (37.24)	29 (31.87)	25 (46.30)		
ECOG (%)				-	0.706
0	69 (47.59)	42 (46.15)	27 (50.00)		
1	74 (51.03)	47 (51.65)	27 (50.00)		
2	2 (1.38)	2 (2.20)	0 (0.00)		
Hypertension (%)				χ^2 = 2.72	0.099
No	103 (71.03)	69 (75.82)	34 (62.96)		
Yes	42 (28.97)	22 (24.18)	20 (37.04)		
Diabetes (%)				χ^2 = 0.45	0.500
No	122 (84.14)	78 (85.71)	44 (81.48)		
Yes	23 (15.86)	13 (14.29)	10 (18.52)		

(*Continued*)

https://doi.org/10.2147/JHC.S580139

Table 1 (Continued).

	Total (n = 145)	Training Set (n = 91)	Validation Set (n = 54)	Statistic	P
Liver cirrhosis (%)				χ^2 = 0.79	0.374
No	66 (45.52)	44 (48.35)	22 (40.74)		
Yes	79 (54.48)	47 (51.65)	32 (59.26)		
Hepatitis (%)				χ^2 = 0.42	0.517
No	31 (21.38)	21 (23.08)	10 (18.52)		
Yes	114 (78.62)	70 (76.92)	44 (81.48)		
BCLC				χ^2 = 0.17	0.684
B	72 (49.66)	44 (48.35)	28 (51.85)		
C	73 (50.34)	47 (51.65)	26 (48.15)		
Antiviral therapy (%)				χ^2 = 0.959	0.327
No	121 (83.45)	81 (89.01)	45 (83.3)		
Yes	24 (16.55)	10 (10.99)	9 (16.7)		
TBIL (umol/L)	22.45 ± 13.37	22.39 ± 14.10	22.54 ± 12.19	t = −0.06	0.949
ALT(U/L)	41.00 (25.00, 59.00)	41.00 (27.50, 58.00)	41.00 (24.25, 60.75)	Z = −0.41	0.681
AST(U/L)	53.00 (38.00, 93.00)	55.00 (41.50, 99.00)	47.00 (32.25, 87.00)	Z = −1.24	0.217
AFP				χ^2 = 0.54	0.762
< 20	41 (28.28)	25 (27.47)	16 (29.63)		
20~400	34 (23.45)	20 (21.98)	14 (25.93)		
> 400	70 (48.28)	46 (50.55)	24 (44.44)		

Abbreviations: t, *t*-test; Z, Mann–Whitney test; χ^2, Chi-square test; -, Fisher exact; SD, standard deviation; M, median; Q_1, 1st quartile; Q_3, 3st quartile; ALT, alanine aminotransferase; AST, aspartate aminotransferase; TBIL, total bilirubin.

Table 2 Comparison of Systemic Inflammatory Indices

	Total (n = 145)	Training Set (n = 91)	Validation Set (n = 54)	Statistic	P
NEU (10^9 /L)	3.62 (2.40, 5.43)	3.72 (2.67, 5.25)	3.54 (2.13, 5.44)	Z = −0.82	0.412
PLT (10^9 /L)	133.00 (84.00, 205.00)	137.00 (93.00, 198.00)	127.50 (79.00, 223.50)	Z = −0.52	0.603
PIVKA-II (mAU /mL)	4170.00 (458.03, 23587.00)	6887.00 (893.00, 29561.00)	3839.69 (867, 30000)	Z = −1.388	0.165
LYM (10^9 /L)	1.12 ± 0.47	1.08 ± 0.46	1.20 ± 0.49	t = −1.43	0.155
MON (10^9 /L)	0.52 ± 0.23	0.52 ± 0.24	0.52 ± 0.21	t = 0.02	0.981
PDW(fl)	14.70 (13.00, 16.70)	14.40 (12.45, 16.40)	15.00 (13.2, 16.7)	Z = −1.387	0.166
RBC (10^{12} /L)	4.15 ± 0.72	4.16 ± 0.74	4.14 ± 0.70	t = 0.20	0.844
RDW (%)	13.80 ± 2.44	13.66 ± 1.72	14.04 ± 3.32	t = −0.91	0.364
LMR	2.42 ± 1.26	2.29 ± 1.01	2.63 ± 1.60	t = −1.55	0.123
NLR	3.35 (2.25, 5.35)	3.46 (2.48, 5.53)	3.09 (1.88, 4.90)	Z = −1.26	0.206
PLR	132.14 (85.71, 197.00)	142.31 (93.45, 196.05)	117.77 (74.53, 199.29)	Z = −1.29	0.198
SIRI	1.60 (1.01, 2.72)	1.61 (1.12, 2.82)	1.48 (0.93, 2.52)	Z = −1.01	0.311
SII	475.16 (246.86, 853.10)	477.29 (261.43, 869.77)	441.96 (206.04, 736.78)	Z = −1.19	0.236

Abbreviations: t, *t*-test; Z, Mann–Whitney test; χ^2, Chi-square test; -, Fisher exact; SD, standard deviation; M, median; Q_1, 1st quartile; Q_3, 3st quartile; NEU, neutrophil; PLT, platelet; NLR, neutrophil-to-lymphocyte ratio; LYM, lymphocytes; MON, monocytes; PDW, platelet distribution width; RBC, red blood cells; LMR, lymphocyte-to-monocyte ratio; PLR, platelet-to-lymphocyte ratio; SIRI, systemic inflammation response index; SII, systemic immune-inflammation index.

Development of an ORR Prediction Model for Triplet Therapy

Based on the univariate analysis and LASSO-selected features, AFP level, tumor rupture, tumor number, LMR, irregular arterial enhancement, and PVTT were incorporated into a multivariate logistic regression model to identify independent predictors and construct a predictive nomogram. As summarized in Table 5, all six variables were confirmed as independent factors significantly associated with treatment response. The model demonstrated good fit without over-fitting, as indicated by the Hosmer–Lemeshow test (χ^2 = 6.178, P = 0.627). Consequently, these six predictors were used to develop a model for estimating the ORR following triple therapy in the training cohort.

Table 3 Comparison of Baseline Radiological Characteristics

	Total (n = 145)	Training Set (n = 91)	Validation Set (n = 54)	Statistic	P
Tumor number (%)				χ^2 = 1.86	0.172
Single	39 (26.90)	28 (30.77)	11 (20.37)		
Multiple	106 (73.10)	63 (69.23)	43 (79.63)		
Tumor diameter (mm)	85.95 ± 37.73	88.90 ± 40.32	80.96 ± 32.67	t = 1.23	0.222
Liver hemorrhage (%)				χ^2 = 0.58	0.446
No	80 (55.17)	48 (52.75)	32 (59.26)		
Yes	65 (44.83)	43 (47.25)	22 (40.74)		
PVTT (%)				χ^2 = 0.79	0.374
No	79 (54.48)	47 (51.65)	32 (59.26)		
Yes	66 (45.52)	44 (48.35)	22 (40.74)		
Metastasis (%)				χ^2 = 0.03	0.871
No	109 (75.17)	68 (74.73)	41 (75.93)		
Yes	36 (24.83)	23 (25.27)	13 (24.07)		
Tumor Morphology (%)				χ^2 = 1.66	0.436
Nodular	56 (38.62)	32 (35.16)	24 (44.44)		
Massive	49 (33.79)	31 (34.07)	18 (33.33)		
Diffuse	40 (27.59)	28 (30.77)	12 (22.22)		
Capsule (%)				χ^2 = 3.24	0.072
No	94 (64.83)	64 (70.33)	30 (55.56)		
Yes	51 (35.17)	27 (29.67)	24 (44.44)		
Arterial phase enhancement (%)				χ^2 = 1.44	0.230
No	63 (43.45)	43 (47.25)	20 (37.04)		
Yes	82 (56.55)	48 (52.75)	34 (62.96)		
Tumor Location (%)				χ^2 = 0.14	0.713
Unilobar	70 (48.28)	45 (49.45)	25 (46.30)		
Bilobar	75 (51.72)	46 (50.55)	29 (53.70)		

Model Comparison and Selection

To validate and evaluate the performance of the comprehensive model, we developed three distinct models: the Combined Model (incorporating AFP, LMR, tumor rupture, tumor number, irregular arterial enhancement, and PVTT), the Clinical Model (comprising AFP and LMR), and the Imaging Model (including tumor rupture, tumor number, irregular arterial enhancement, and PVTT) (Table 6). Results from the training set demonstrated that the Combined Model achieved significantly higher predictive accuracy compared to both the Clinical and Imaging Models. This

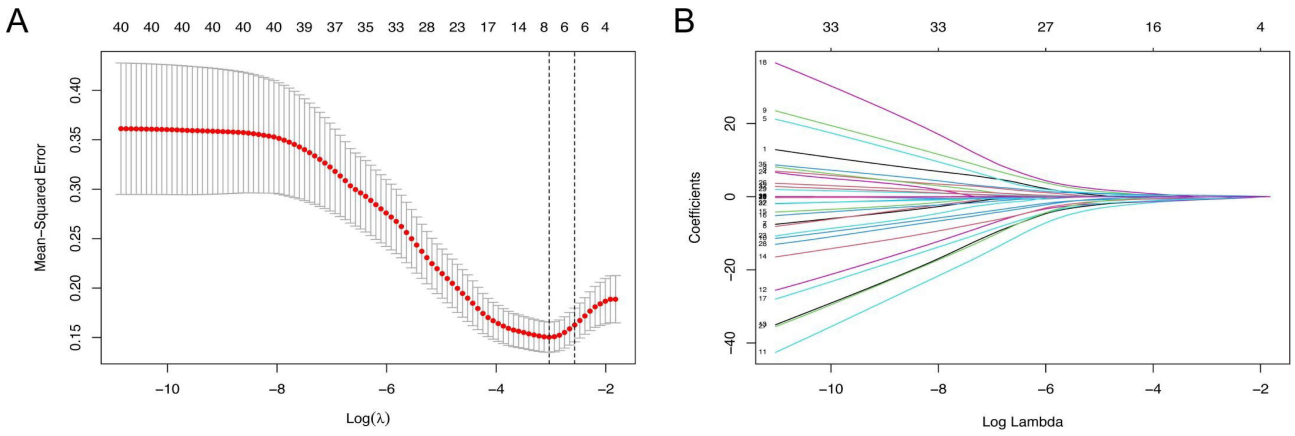

Figure 2 LASSO cox regression analysis on the independent variables (**A** and **B**).

https://doi.org/10.2147/JHC.S580139

Table 4 Univariate Analysis of Predictors for Objective Response to Triple Therapy

	Total (n = 91)	PD+SD (n = 69)	PR+CR (n = 22)	Statistic	P
LYM (10^9 /L)	1.08 ± 0.46	1.05 ± 0.45	1.18 ± 0.49	t = −1.16	0.247
MON (10^9 /L)	0.52 ± 0.24	0.54 ± 0.24	0.44 ± 0.19	t = 1.84	0.069
PDW(fl)	14.40 (12.45, 16.40)	14.40 (12.20, 16.40)	14.00 (13.05, 17.10)	Z = −0.59	0.556
RBC (10^{12} /L)	4.16 ± 0.74	4.18 ± 0.77	4.11 ± 0.66	t = 0.39	0.694
RDW (%)	13.66 ± 1.72	13.84 ± 1.87	13.10 ± 1.01	t = 1.76	0.081
TBIL (umol/L)	22.39 ± 14.10	23.87 ± 15.52	17.75 ± 6.46	t = 1.80	0.076
Tumor diameter(mm)	88.90 ± 40.32	90.97 ± 41.83	82.41 ± 35.25	t = 0.87	0.389
ALT (U/L)	41.00 (27.50, 58.00)	40.00 (27.00, 55.00)	44.50 (32.25, 66.00)	Z = −0.61	0.544
AST (U/L)	55.00 (41.50, 99.00)	71.00 (44.00, 110.00)	47.00 (29.25, 55.00)	Z = −2.46	0.014
NEU (10^9 /L)	3.72 (2.67, 5.25)	3.68 (2.79, 5.43)	3.87 (2.52, 4.29)	Z = −0.68	0.496
PLT (10^9 /L)	137.00 (93.00, 198.00)	133.00 (84.00, 199.00)	138.00 (107.25, 186.75)	Z = −0.40	0.687
PIVKA-II (mAU /mL)	6887.00 (893.00, 29561.00)	6987.00 (1090.00, 30163.00)	2148.50 (254.25, 14947.00)	Z = −1.47	0.142
LMR	2.29 ± 1.01	2.08 ± 0.82	2.96 ± 1.25	t = −3.84	<0.001
NLR	3.46 (2.48, 5.53)	3.84 (2.62, 5.72)	2.83 (2.05, 3.54)	Z = −1.84	0.065
PLR	142.31 (93.45, 196.05)	141.38 (94.14, 197.00)	142.37 (89.66, 173.48)	Z = −0.41	0.683
SIRI	1.61 (1.12, 2.82)	1.73 (1.18, 2.94)	1.48 (0.83, 1.91)	Z = −1.91	0.056
SII	477.29 (261.43, 869.77)	477.29 (288.61, 921.96)	519.35 (218.73, 807.20)	Z = −0.47	0.636
AFP				χ^2 = 14.59	<0.001
< 20	25 (27.47)	12 (17.39)	13 (59.09)		
20~400	20 (21.98)	17 (24.64)	3 (13.64)		
> 400	46 (50.55)	40 (57.97)	6 (27.27)		
Tumor number (%)				χ^2 = 10.93	<0.001
Single	28 (30.77)	15 (21.74)	13 (59.09)		
Multiple	63 (69.23)	54 (78.26)	9 (40.91)		
Liver hemorrhage (%)				χ^2 = 9.84	0.002
No	48 (52.75)	30 (43.48)	18 (81.82)		
Yes	43 (47.25)	39 (56.52)	4 (18.18)		
PVTT (%)				χ^2 = 5.16	0.023
No	47 (51.65)	31 (44.93)	16 (72.73)		
Yes	44 (48.35)	38 (55.07)	6 (27.27)		
Metastasis (%)				χ^2 = 4.02	0.119
No	68 (74.73)	48 (69.57)	20 (90.91)		
Yes	23 (25.27)	21 (30.43)	2 (9.09)		
Tumor Morphology (%)				χ^2 = 0.93	0.629
Nodular	32 (35.16)	23 (33.33)	9 (40.91)		
Massive	31 (34.07)	23 (33.33)	8 (36.36)		
Diffuse	28 (30.77)	23 (33.33)	5 (22.73)		
Capsule (%)				χ^2 = 0.06	0.800
No	64 (70.33)	49 (71.01)	15 (68.18)		
Yes	27 (29.67)	20 (28.99)	7 (31.82)		
Arterial phase enhancement (%)				χ^2 = 7.55	0.006
No	43 (47.25)	27 (39.13)	16 (72.73)		
Yes	48 (52.75)	42 (60.87)	6 (27.27)		
Tumor Location (%)				χ^2 = 0.00	0.953
Unilobar	45 (49.45)	34 (49.28)	11 (50.00)		
Bilobar	46 (50.55)	35 (50.72)	11 (50.00)		

Abbreviations: t, *t*-test; Z, Mann–Whitney test; χ^2, Chi-square test; -, Fisher exact; SD, standard deviation; M, median; Q_1, 1st Quartile, Q_3: 3st quartile; CR, complete remission; PR, partial remission; SD, stable disease; PD, progressive disease.

superior performance was consistently observed in the validation set (Figures 3A and B). Based on these comprehensive findings, the Combined Model was selected as the optimal predictor of treatment response for patients receiving combination therapy (Figure 3C).

Table 5 Multivariate Analysis of Predictors for Objective Response to Triple Therapy

	B	Se	Wald	P	OR	95% CI of OR	
						Lower	Upper
AFP 20~400	−0.918	1.016	0.817	0.366	0.399	0.054	2.924
AFP > 400	−1.823	0.803	5.161	0.023	0.161	0.033	0.779
Tumor number	−1.712	0.754	5.161	0.023	0.18	0.041	0.791
Liver hemorrhage	−1.713	0.857	3.995	0.046	0.18	0.034	0.967
PVTT	−2.033	0.82	6.141	0.013	0.131	0.026	0.654
Arterial phase enhancement	−1.607	0.771	4.342	0.037	0.2	0.044	0.909
LMR	0.798	0.396	4.069	0.044	2.222	1.023	4.825
Constants	1.044	1.29	0.655	0.418	2.84		

Table 6 ROC Curve Performance of the Three Models

Variable	Training Set			Validation Set		
	AUC	SE	95% CI	AUC	SE	95% CI
Combined Model	0.915	0.0375	0.838–0.963	0.933	0.0332	0.831–0.983
Clinical Model	0.805	0.0568	0.708–0.880	0.883	0.0494	0.766–0.954
Imaging Model	0.872	0.0365	0.785–0.933	0.786	0.086	0.653–0.886

Model Performance and Validation

As shown in Figure 4A, the Combined model demonstrated high predictive accuracy in the training cohort, with an AUC of 0.915 (95% CI, 0.838 to 0.963) and strong discrimination. In the validation cohort (Figure 4B), the nomogram exhibited an AUC of 0.933 (95% CI, 0.831 to 0.963), demonstrating consistently strong predictive performance. These results indicate that the model performed well in the validation cohort as well. Additionally, the calibration curve closely aligned with the ideal 45° line, suggesting that the nomogram's predictions of treatment efficacy were highly consistent with the actual measurements across time points (Figure 4C). For the external test set, the nomogram we developed accurately predicted treatment efficacy (Figure 4D). DCA (Figures 4E and F) demonstrated that the nomogram conferred a positive net benefit across threshold probabilities from approximately 15% to 80%, supporting its utility in guiding treatment decisions.

Assessment of Safety

During treatment with TACE in combination with lenvatinib and an immune checkpoint inhibitor, patients experienced adverse events of varying grades. As shown in Table 7, there were no statistically significant differences in the incidence of adverse events among the three groups ($P > 0.05$), indicating a comparable safety profile across the three combination regimens.

Discussion

HCC remains a leading cause of cancer-related mortality worldwide. While surgical resection offers a potential cure for early-stage disease, the frequently asymptomatic nature of early HCC often leads to diagnosis at advanced, unresectable stages. For these patients, combination therapies involving locoregional and systemic agents have become a cornerstone of treatment, with some achieving sufficient downstaging to become eligible for curative-intent resection.[20] Since its initial report by Goldstein et al in 1976,[21] TACE has been established as a standard locoregional therapy for patients with u-HCC. TACE induces tumor necrosis by occluding the arterial blood supply; however, the resultant hypoxia can paradoxically upregulate pro-angiogenic factors like vascular endothelial growth factor (VEGF), promoting revascularization and the development of collateral circulation, which ultimately limits its long-term efficacy.[22] Consequently, combining TACE with other therapeutic modalities is crucial to improve outcomes.

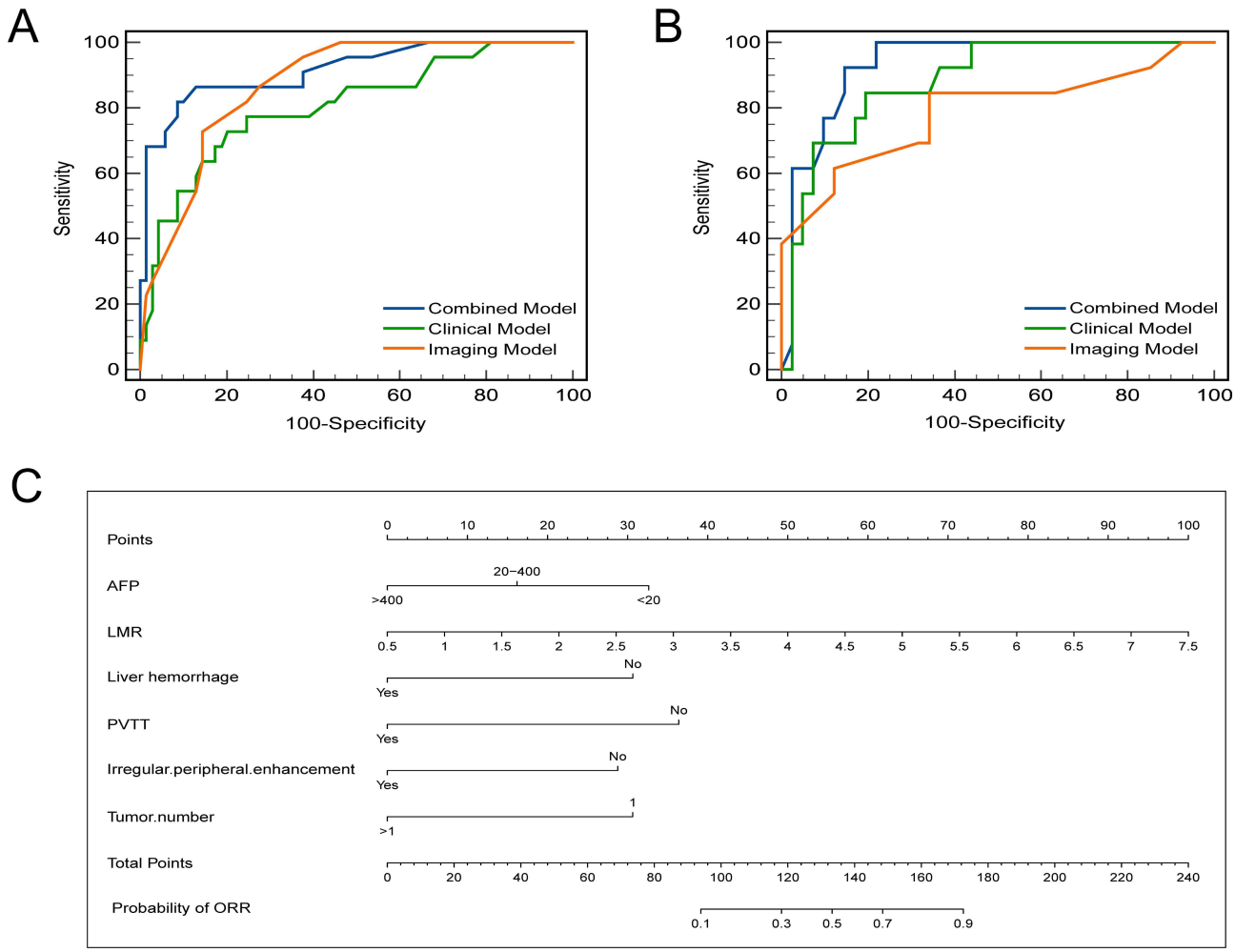

Figure 3 ROC curves of the three models in the in the Training Set (**A**) and Validation Set (**B**). Nomogram for predicting the ORR to triple therapy (**C**).

Recent breakthroughs in targeted therapy and immunotherapy have revolutionized the management of HCC. Targeted agents, such as lenvatinib, inhibit tyrosine kinases involved in angiogenesis, potentially counteracting the hypoxia-induced VEGF surge post-TACE.[23] Conversely, immune checkpoint inhibitors (eg PD-1 inhibitors) block the PD-1/PD-L1 pathway, synergizing with tumor-associated antigens released by TACE to enhance anti-tumor immunity.[24] The immunosuppressive tumor microenvironment (TME) plays a critical role, where factors like VEGF-A derived from tumor-associated macrophages can recruit immunosuppressive cells and induce Fas ligand expression on endothelial cells, inhibiting T-cell infiltration.[25,26] Antiangiogenic therapy may reverse this immunosuppressive TME via vascular normalization, potentiating T-cell-mediated immunity. Thus, a strong rationale exists for the synergistic triple combination of TACE, lenvatinib, and PD-1 inhibitors. The LAUNCH trial[27] demonstrated that TACE plus lenvatinib significantly improved outcomes over lenvatinib alone in advanced HCC, a finding corroborated in real-world studies.[28,29] As triple therapy gains traction, the critical challenge lies in identifying patients most likely to benefit, underscoring the need for predictive biomarkers.

This study developed and validated a non-invasive predictive model integrating radiological features, peripheral blood inflammatory indices, and tumor markers to estimate the likelihood of treatment response in u-HCC patients receiving triple therapy. Our analysis identified AFP level, LMR, presence of PVTT, tumor number, irregular rim-like enhancement on the arterial phase, and tumor rupture as independent predictors of treatment efficacy. The combined model, incorporating these six factors, demonstrated superior predictive performance compared to models based solely on clinical or imaging features, with AUC values of 0.915 and 0.933 in the training and validation cohorts, respectively. Calibration curves and DCA further confirmed the model's robust accuracy and clinical utility.

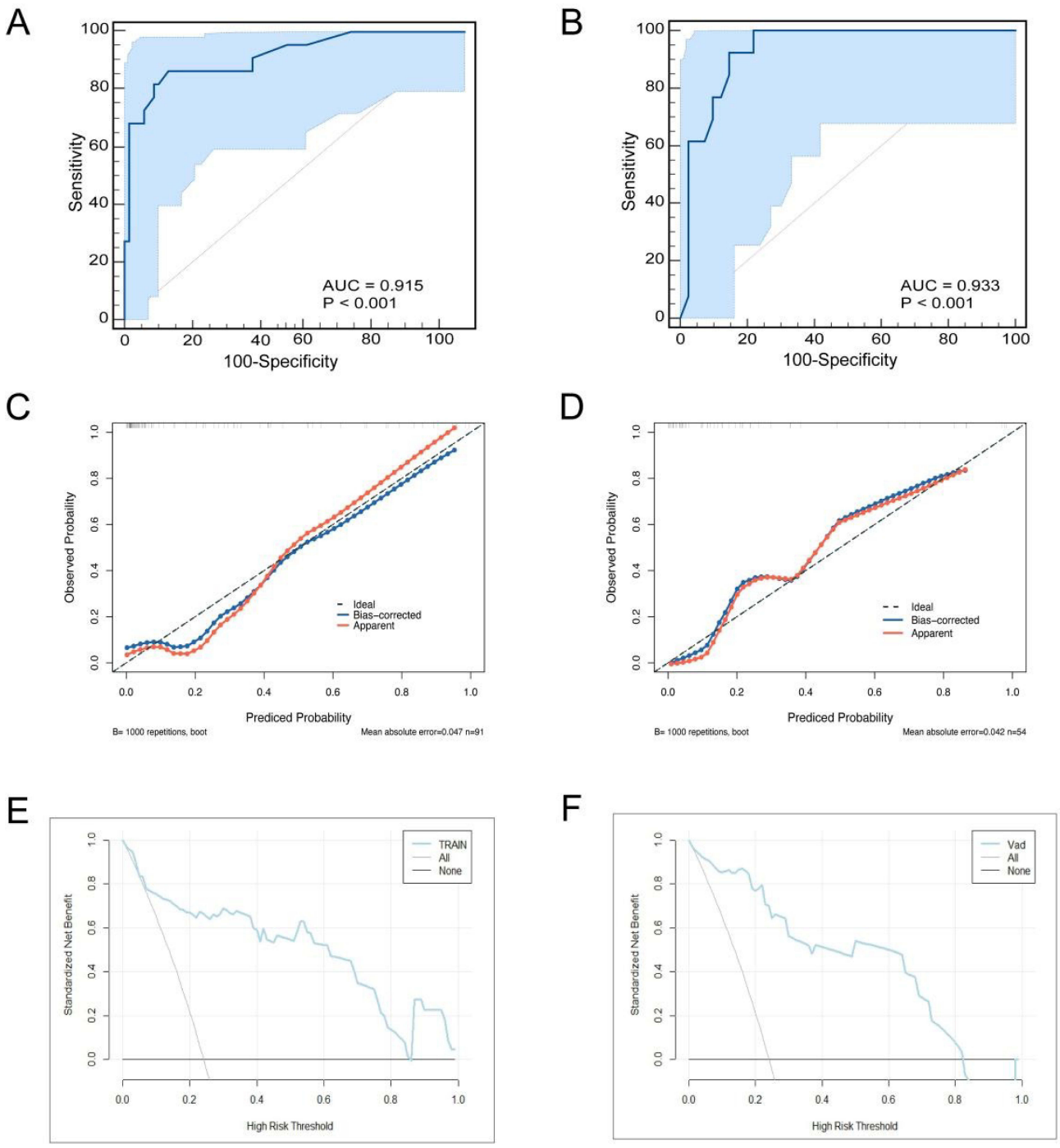

Figure 4 Nomogram for predicting non-response to triple therapy roc curves in training (**A**) and validation (**B**) sets. Calibration curve of radiomics nomogram in training (**C**) and validation (**D**) sets. Decision curve analysis of radiomics nomogram in training (**E**) and validation (**F**) sets.

The prognostic significance of the identified predictors can be interpreted through their interconnected biological and clinical implications within the tumor microenvironment (TME) framework. Elevated AFP not only reflects tumor burden but may also promote an immunosuppressive TME via VEGF-mediated pathways. A decreased LMR often signifies a systemic inflammatory shift towards protumorigenic monocytes (M2 macrophages) and diminished lymphocyte activity. Notably, imaging features such as PVTT and irregular arterial enhancement are hallmarks of aberrant angiogenesis, which fosters a hypoxic, immune-excluded TME conducive to disease progression and potentially suboptimal response to therapy.[30] Multiple tumors suggest intrahepatic dissemination or heterogeneity, complicating

https://doi.org/10.2147/JHC.S580139

Table 7 Comparison of Adverse Events Across Different Treatment Regimens

	Total (n = 145)	Adverse Events (%)
TACE + Lenvatinib + Camrelizumab	30	18 (60%)
TACE + Lenvatinib + Tislelizumab	62	41 (66.13%)
TACE + Lenvatinib + Sintilimab	53	26 (49.06%)
χ^2		3.463
P		0.177

locoregional treatment efficacy. Tumor rupture incites pro-inflammatory cascades that may paradoxically modulate immune responses. Regarding safety in patients with PVTT, while our cohort did not show a significant increase in severe adverse events (eg, major bleeding or thrombosis), the inherent risks associated with macrovascular invasion warrant vigilant monitoring in clinical practice, as supported by existing literature.[31]

Our triple therapy strategy is mechanistically poised to counteract these adverse TME features: TACE induces tumor necrosis and antigen release, lenvatinib normalizes vasculature and mitigates immunosuppression, and anti-PD-1 agents reinvigorate T-cell immunity. Thus, our predictive model essentially identifies patients whose underlying TME and tumor biology are most amenable to this multimodal attack.

Regarding the treatment regimens, our study employed lenvatinib combined with three different PD-1 inhibitors (camrelizumab, sintilimab, and tislelizumab). The results indicated no statistically significant differences in efficacy or safety profiles among the three combinations, suggesting comparable therapeutic effects when these agents are paired with lenvatinib. This observation aligns with previous studies reporting similar efficacy across different PD-1/PD-L1 inhibitors in combination with antiangiogenic therapy.[6] Although structural differences exist among these agents, their shared mechanism of action—blockading the PD-1/PD-L1 axis to reactivate T-cell immunity—likely underlies the comparable synergistic effects observed with lenvatinib.

Several limitations of this study should be acknowledged. First, the restrictive inclusion criteria (treatment-naïve patients receiving no other antitumor therapies) resulted in a relatively limited sample size from a single geographic region, potentially introducing selection bias and limiting generalizability. Consequently, adequately powered subgroup analyses (eg, by tumor size or liver function) were precluded, and the impact of dynamic biomarker changes during treatment could not be assessed—both of which might refine predictive accuracy in specific subpopulations. Second, unmeasured confounding factors inherent to retrospective studies may exist. Third, although imaging assessments were standardized, some subjectivity is inevitable, and our model did not incorporate advanced radiographic biomarkers (eg, tumor-induced vascular compression) that may predict microvascular invasion and satellite nodules.[31] Fourth, the primary endpoint was short-term radiological response (ORR); longer-term outcomes such as overall survival and progression-free survival remain to be evaluated.

Future studies should address these limitations. Specifically, prospective, multi-center validation in larger and more heterogeneous cohorts is essential to confirm generalizability across diverse populations and settings, which would also address the observed performance consistency between training and external validation sets. This expanded validation would also enable robust subgroup analyses. Incorporating serial biomarker measurements and advanced imaging features (eg, vascular compression) may enhance dynamic prediction. Moreover, integrating radiomics, deep learning, or liquid biopsies could uncover novel biomarkers. Ultimately, validating this tool against long-term survival outcomes and exploring its utility in guiding personalized combination strategies within the triple-therapy framework are critical next steps.

In conclusion, we have developed and validated a practical, non-invasive nomogram that integrates routinely available clinical, inflammatory, and radiological biomarkers. This tool demonstrates high accuracy in predicting response to TACE-based triple therapy in u-HCC patients prior to treatment initiation. Upon further validation, it holds significant potential to aid clinicians in personalizing therapeutic strategies, thereby optimizing outcomes and avoiding unnecessary toxicity in patients unlikely to benefit.

Data Sharing Statement

All data generated or analyzed in this study are included in this published article.

Ethics Approval and Consent to Participate

This study was conducted in accordance with the Declaration of Helsinki (2013 revision) and was approved by the Ethics Committee of Yancheng Tinghu District People's Hospital (Approval No.: 2024-SR-016). The need for informed consent was waived by the Ethics Committee due to the retrospective nature of the study, which involved no more than minimal risk to the participants. All patient data were anonymized and maintained with strict confidentiality to protect patient privacy.

Author Contributions

All authors made a significant contribution to the work reported, whether that is in the conception, study design, execution, acquisition of data, analysis and interpretation, or in all these areas; took part in drafting, revising or critically reviewing the article; gave final approval of the version to be published; have agreed on the journal to which the article has been submitted; and agree to be accountable for all aspects of the work.

Funding

This research was supported by the following funding: 1. Yancheng City Basic Research Program (General Project) (No. YCBK2024099); 2. Jiangsu Vocational College of Medicine University-Local Collaborative Innovation Project (No. 202491601).

Disclosure

The authors declare no competing interests.

References

1. Sung H, Ferlay J, Siegel RL, et al. Global cancer statistics 2020: GLOBOCAN estimates of incidence and mortality worldwide for 36 cancers in 185 countries. *Ca A Cancer J Clin*. 2021;71(3):209–249. doi:10.3322/caac.21660
2. Forner A, Reig M, Bruix J. Hepatocellular carcinoma. *Lancet*. 2018;391(10127):1301–1314. doi:10.1016/s0140-6736(18)30010-2
3. Bray F, Ferlay J, Soerjomataram I, Siegel RL, Torre LA, Jemal A. Global cancer statistics 2018: GLOBOCAN estimates of incidence and mortality worldwide for 36 cancers in 185 countries. *CA Cancer J Clin*. 2018;68(6):394–424. doi:10.3322/caac.21492
4. Zhang J, Zhang X, Mu H, et al. Surgical conversion for initially unresectable locally advanced hepatocellular carcinoma using a triple combination of angiogenesis inhibitors, anti-PD-1 antibodies, and hepatic arterial infusion chemotherapy: a retrospective study. *Front Oncol*. 2021;11:729764. doi:10.3389/fonc.2021.729764
5. Huang G, Li PP, Lau WY, et al. Antiviral therapy reduces hepatocellular carcinoma recurrence in patients with low HBV-DNA levels: a randomized controlled trial. *Ann Surg*. 2018;268(6):943–954. doi:10.1097/sla.0000000000002727
6. Sun HC, Zhou J, Wang Z, et al. Chinese expert consensus on conversion therapy for hepatocellular carcinoma (2021 edition). *Hepatobiliary Surg Nutr*. 2022;11(2):227–252. doi:10.21037/hbsn-21-328
7. Kulik L, El-Serag HB. Epidemiology and management of hepatocellular carcinoma. *Gastroenterology*. 2019;156(2):477–491.e1. doi:10.1053/j.gastro.2018.08.065
8. Yang YM, Kim SY, Seki E. Inflammation and liver cancer: molecular mechanisms and therapeutic targets. *Semin Liver Dis*. 2019;39(1):26–42. doi:10.1055/s-0038-1676806
9. Liao R, Jiang N, Tang ZW, et al. Systemic and intratumoral balances between monocytes/macrophages and lymphocytes predict prognosis in hepatocellular carcinoma patients after surgery. *Oncotarget*. 2016;7(21):30951–30961. doi:10.18632/oncotarget.9049
10. Neal CP, Cairns V, Jones MJ, et al. Prognostic performance of inflammation-based prognostic indices in patients with resectable colorectal liver metastases. *Med Oncol*. 2015;32(5):144. doi:10.1007/s12032-015-0590-2
11. Yoneda N, Matsui O, Kobayashi S, et al. Current status of imaging biomarkers predicting the biological nature of hepatocellular carcinoma. *Japanese J Radiol*. 2019;37(3):191–208. doi:10.1007/s11604-019-00817-3
12. Chen X, Yang Z, Deng J. Use of 64-slice spiral CT examinations for hepatocellular carcinoma (DR LU). *J BUON*. 2019;24(4):1435–1440.
13. Wang L, Dong T, Xin B, et al. Integrative nomogram of CT imaging, clinical, and hematological features for survival prediction of patients with locally advanced non-small cell lung cancer. *Eur Radiol*. 2019;29(6):2958–2967. doi:10.1007/s00330-018-5949-2
14. Schwarz L, Bubenheim M, Zemour J, et al. Bleeding recurrence and mortality following interventional management of spontaneous HCC rupture: results of a multicenter European study. *World J Surg*. 2018;42(1):225–232. doi:10.1007/s00268-017-4163-8
15. Liu M, Shi J, Mou T, Wang Y, Wu Z, Shen A. Systematic review of hepatic arterial infusion chemotherapy versus sorafenib in patients with hepatocellular carcinoma with portal vein tumor thrombosis. *J Gastroenterol Hepatol*. 2020;35(8):1277–1287. doi:10.1111/jgh.15010
16. Wang TC, An TZ, Li JX, Pang PF. Systemic inflammation response index is a prognostic risk factor in patients with hepatocellular carcinoma undergoing TACE. *Risk Manag Healthc Policy*. 2021;14:2589–2600. doi:10.2147/rmhp.S316740

17. Schobert IT, Savic LJ, Chapiro J, et al. Neutrophil-to-lymphocyte and platelet-to-lymphocyte ratios as predictors of tumor response in hepatocellular carcinoma after DEB-TACE. *Eur Radiol*. 2020;30(10):5663–5673. doi:10.1007/s00330-020-06931-5
18. Xue TC, Jia QA, Ge NL, et al. The platelet-to-lymphocyte ratio predicts poor survival in patients with huge hepatocellular carcinoma that received transarterial chemoembolization. *Tumour Biol*. 2015;36(8):6045–6051. doi:10.1007/s13277-015-3281-x
19. Li D, Zhao X, Pi X, Wang K, Song D. Systemic immune-inflammation index and the survival of hepatocellular carcinoma patients after transarterial chemoembolization: a meta-analysis. *Clin Exp Med*. 2023;23(6):2105–2114. doi:10.1007/s10238-022-00889-y
20. Yang Y, Chen D, Zhao B, et al. The predictive value of PD-L1 expression in patients with advanced hepatocellular carcinoma treated with PD-1/PD-L1 inhibitors: a systematic review and meta-analysis. *Cancer Med*. 2023;12(8):9282–9292. doi:10.1002/cam4.5676
21. Manjunatha N, Ganduri V, Rajasekaran K, Duraiyarasan S, Adefuye M. Transarterial chemoembolization and unresectable hepatocellular carcinoma: a narrative review. *Cureus*. 2022;14(8):e28439. doi:10.7759/cureus.28439
22. Seki A, Hori S. Switching the loaded agent from epirubicin to cisplatin: salvage transcatheter arterial chemoembolization with drug-eluting microspheres for unresectable hepatocellular carcinoma. *Cardiovasc Intervent Radiol*. 2012;35(3):555–562. doi:10.1007/s00270-011-0176-0
23. Zhong BY, Jin ZC, Chen JJ, Zhu HD, Zhu XL. Role of transarterial chemoembolization in the treatment of hepatocellular carcinoma. *J Clin Transl Hepatol*. 2023;11(2):480–489. doi:10.14218/jcth.2022.00293
24. Cheu JW, Wong CC. Mechanistic rationales guiding combination hepatocellular carcinoma therapies involving immune checkpoint inhibitors. *Hepatology*. 2021;74(4):2264–2276. doi:10.1002/hep.31840
25. Li H, You J, Wei Y, et al. Huaier improves the efficacy of anti-PD-L1 Ab in the treatment of hepatocellular carcinoma by regulating tumor immune microenvironment. *Phytomedicine*. 2024;123:155189. doi:10.1016/j.phymed.2023.155189
26. Mohammadnezhad G, Noqani H, Rostamian P, Sattarpour M, Arabloo J. Lenvatinib in the treatment of unresectable hepatocellular carcinoma: a systematic review of economic evaluations. *Eur J Clin Pharmacol*. 2023;79(7):885–895. doi:10.1007/s00228-023-03502-7
27. Peng Z, Fan W, Zhu B, et al. Lenvatinib combined with transarterial chemoembolization as first-line treatment for advanced hepatocellular carcinoma: a Phase III, randomized clinical trial (LAUNCH). *J Clin Oncol*. 2023;41(1):117–127. doi:10.1200/jco.22.00392
28. Zhu HD, Li HL, Huang MS, et al. Transarterial chemoembolization with PD-(L)1 inhibitors plus molecular targeted therapies for hepatocellular carcinoma (CHANCE001). *Signal Transduct Target Ther*. 2023;8(1):58. doi:10.1038/s41392-022-01235-0
29. Li S, Wu J, Wu J, et al. Prediction of early treatment response to the combination therapy of TACE plus lenvatinib and anti-PD-1 antibody immunotherapy for unresectable hepatocellular carcinoma: multicenter retrospective study. *Front Immunol*. 2023;14:1109771. doi:10.3389/fimmu.2023.1109771
30. Wang QB, Luo WL, Li YK, et al. Tumor compression of the hepatic or portal vein predicts the presence of microvascular invasion and satellite nodules in hepatocellular carcinoma: a retrospective study. *J Hepatocell Carcinoma*. 2025;12:2055–2067. doi:10.2147/jhc.S544589
31. Wang QB, Li J, Zhang ZJ, et al. The effectiveness and safety of therapies for hepatocellular carcinoma with tumor thrombus in the hepatic vein, inferior vena cave and/or right atrium: a systematic review and single-arm meta-analysis. *Expert Rev Anticancer Ther*. 2025;25(5):561–570. doi:10.1080/14737140.2025.2489651